Journal of Marine Systems, 4 (1993) 117–132
Elsevier Science Publishers B.V., Amsterdam

Flux measurements from a SWATH ship in SWADE

Kristina B. Katsaros [a], Mark A. Donelan [b] and William M. Drennan [b]

[a] *Department of Atmospheric Sciences AK-40, University of Washington, Seattle, WA 98195, USA*
[b] *National Water Research Institute, Canada Centre for Inland Waters, 867 Lakeshore Road, P.O. Box 5050, Burlington, Ontario L7R 4A6, Canada*

(Received October 27, 1992; revised and accepted February 5, 1993)

ABSTRACT

Katsaros, K.B., Donelan, M.A. and Drennan, W.M., 1993. Flux measurements from a SWATH ship in SWADE. J. Mar. Syst., 4: 117–132.

The Surface Wave Dynamics Experiment (SWADE) took place east of the U.S. Coast in the winter of 1990–1991. A major objective of the research program is to refine our understanding of the relationship between fluxes to the sea surface and the sea state as determined from directional wave spectra. Simultaneous measurements of turbulent fluxes of mass, momentum and energy between sea and air, with the directional wave spectra, were required to meet this objective. In this short article we describe the process of obtaining turbulent flux measurements from a small water-plane-area twin hull (SWATH) ship. We measured turbulent fluxes of momentum, heat and water vapor from a tall mast at the bow of the SWATH ship *Frederick G. Creed* by the eddy correlation method, while the ship was moving into the wind. Directional wave spectra were obtained from a wave staff array ahead of the bow of the ship. The motion of the ship was recorded and a coordinate rotation was performed for each data sample. After all instrument response and motion corrections have been accounted for, we compare our calculated turbulent fluxes with values computed from another standard method, viz. the inertial dissipation method. This approach is not susceptible to platform motion but relies on assumptions that are not always valid. However, the two methods agree on average within 12%, 20% and 31% for momentum, water vapor and heat fluxes, respectively.

Introduction

The Surface Wave Dynamics Experiment (SWADE) took place off the east coast of the United States in the region 35°N to 42°N and 70°W to 76°W, during the period from October 1990 to March 1991. The objectives of SWADE include the direct measurement of wind stress and sensible and latent heat fluxes, in conjunction with detailed measurements of the sea state, for analysis of the relationship between variability in the fluxes and the sea state (Weller et al., 1991). Measurements of wind stress and directional wave spectra were obtained from several platforms including moored buoys (Anctil et al., 1993), aircraft and a small ship. In this article we limit ourselves to the process of deriving turbulent fluxes from measurements made on the small ship while under way in the region shown in Fig. 1.

Wave growth depends on the rate of momentum transfer from the atmosphere to the sea, τ_o. This stress varies with the speed of the wind, the stratification of the atmosphere and the "roughness" of the sea. The roughness is usually defined in terms of a roughness length, z_o, a scaling parameter, that is the velocity origin of the logarithmic wind profile over a surface. It is known that z_o depends on the "state of the sea", which we define in terms of a significant wave height and the inverse wave age, the ratio between the wind speed at 10 m, U_{10}, and the phase velocity of the waves at the peak of the spectrum, C_p. U_{10}/C_p is thus a relative measure of the force of the wind. The currently available relationships between τ_o, z_o, and U_{10}/C_p only apply to simple

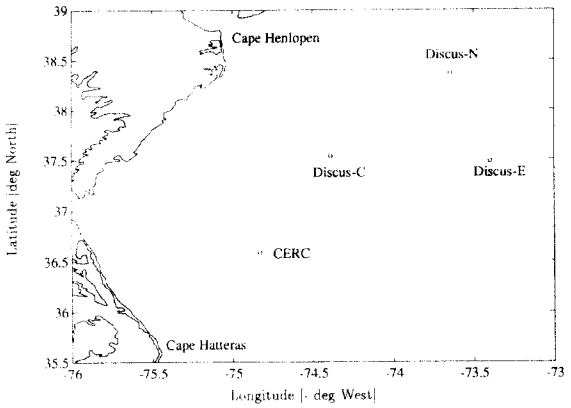

Fig. 1. The SWADE experiment area where the *Frederick G. Creed* operated during IOP2 and IOP3, showing wave directional and meteorological buoy-locations.

conditions of wind waves, whose travel direction is closely aligned with the wind direction (Donelan, 1990; Smith et al., 1992). In SWADE we sought to define the more complex situations which have to be analyzed with the use of numerical wave models. Because of the many variables in the atmosphere and the ocean that can influence the wind stress–sea state relationship and the development of waves, e.g., atmospheric mesoscale and synoptic scale circulations, ocean currents and sea surface temperature variability, SWADE was planned to cover a long time period with continuous measurements made from moored buoys in several locations and from occa-

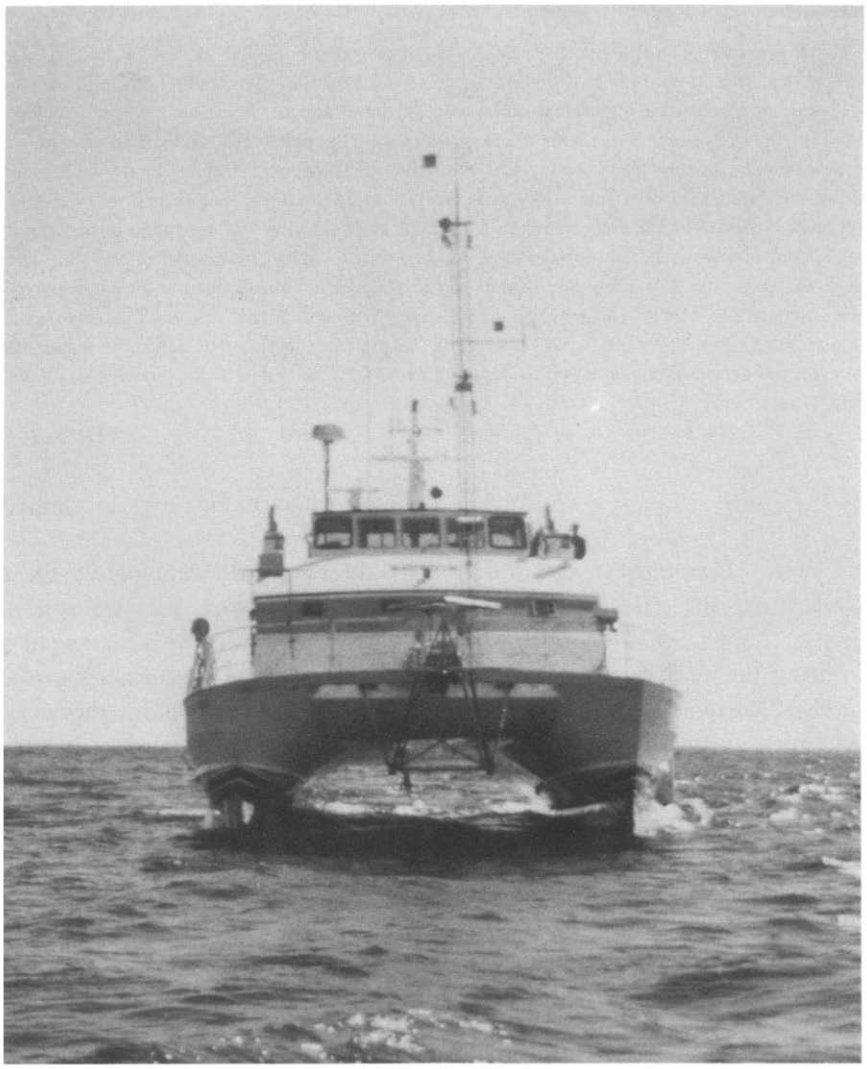

Fig. 2. Photograph of the *Frederick G. Creed*.

sional aircraft missions with remote sensing devices that determine the variability of the sea state over a large area.

A stabilized spar buoy, ideal for obtaining atmospheric turbulence measurements at sea, was lost early in the experiment. Since the measurements were particularly complete from this buoy the loss was damaging to the program as a whole. Replacement instruments were available, so a substitute platform, a relatively stable small ship was quickly brought to the field site. The *Frederick G. Creed* (Fig. 2) is a "small water-plane area twin hull" (SWATH) ship that causes minimal interference with waves. It is 20 m long and its superstructure measures only 6.7 m above the sea. In this article we describe the instrumentation and the analysis procedures for obtaining the turbulent fluxes of momentum, heat and water vapor by the eddy correlation method from a moving platform such as a SWATH ship. The *Frederick G. Creed* participated during two intensive observing periods, each about two weeks in duration, January and February 22–March 9 (IOP3).

Theory

The correlations between fluctuations in vertical air velocity, w and fluctuations in one of the three atmospheric parameters: horizontal wind speed, u, atmospheric temperature, t, or humidity, q, when averaged over an appropriate time interval, produce the net transport of these quantities in the vertical by turbulent eddies. The surface wind stress, τ, the heat flux, H, and the evaporation rate from the sea, E, are related to these covariances through:

$$\tau = -\rho\overline{u'w'} \tag{1}$$

$$H = \rho c_p \overline{w'T'} \tag{2}$$

$$E = \rho\overline{w'q'} \tag{3}$$

where ρ is density and c_p is specific heat at constant pressure.

For these so-called direct measurements of turbulent fluxes, obtaining earth referenced velocity fluctuations accurately is the main difficulty on a moving platform. The problem is particularly severe for the momentum flux, because any misalignment of the coordinate system of the velocity measuring instrument with the earth-based coordinate system causes "cross-talk" between horizontal and vertical wind components. A part of the fluctuations in measured u and w are then perfectly correlated. To determine the turbulent fluxes from a platform with large tilts and accelerations using the eddy correlation technique, the motion of the platform has to be measured and removed from the signal at each time step. To this end, a motion sensing package was installed on the SWATH ship. Although such direct measurements have been made in the past (Mitsuta and Fujitani, 1974; Bradley et al., 1991) it was assumed that either all or part of the ship motion could be neglected. In particular, Mitsuta and Fujitani neglected linear ship acceleration (heave, surge and sway) in their analyses while Bradley et al., for their measurements in the tropics, considered all ship motion to be negligible.

A second method for obtaining the turbulent fluxes is to assume equivalence between production and dissipation of turbulence. Then, by measuring the turbulence at high frequencies where the cascade of energy from low to high frequencies occurs (from large to small scales), one can *infer* the turbulent flux (e.g., Large and Pond, 1982; Fairall and Larsen, 1986). The actual dissipation happens at very high frequencies, which are extremely difficult to measure. Thus we analyze for the spectral level in the so-called inertial subrange, where the auto-spectra of u, v, w, T and q have a $-5/3$ slope with respect to frequency. This method is considered indirect and is subject to large corrections when buoyancy forces influence the turbulence levels. Furthermore, there is approximately 20% uncertainty in the empirical Kolmogorov constants (Large and Pond, 1982; Fairall and Larsen, 1986).

The motion of a ship occurs at relatively low frequencies and it has therefore been suggested that the higher frequencies in the inertial subrange are unaffected and the "inertial dissipation method" can be used to determine turbulent fluxes from moving platforms at sea. We compare eddy correlation and inertial dissipation estimates of the turbulent fluxes in the Results section.

The measurement devices

For meteorological measurements during winter on the high seas, special rugged sensors are required that do not need regular cleaning and can continue to function during and after precipitation. All the meteorological sensors were mounted on a 9 m tall mast on the foredeck of the *Frederick G. Creed* (Fig. 3). The instruments were mounted on the mast while we were in port and could not be adjusted while at sea for safety reasons. The motion of the ship was recorded by several sensors providing redundancy. These were contained in a motion sensing package which was at the bow of the ship near the meteorological mast and the wave staff array.

Motion sensors

The ability to measure the motion of the ship correctly is of paramount importance in recovering accurate estimates of the turbulent fluxes. Consequently, all six degrees of translation and rotation of the ship were measured by duplicate sensors and the twelve signals were recorded continuously. In addition to providing the assurance of redundancy in case of failures, the parallel recordings can be used in duplicate calculations as a check on the accuracy of the method of motion correction.

The translational and rotational motion of the ship was measured by a pair of tri-axial sets of linear accelerometers (surge, sway and heave)

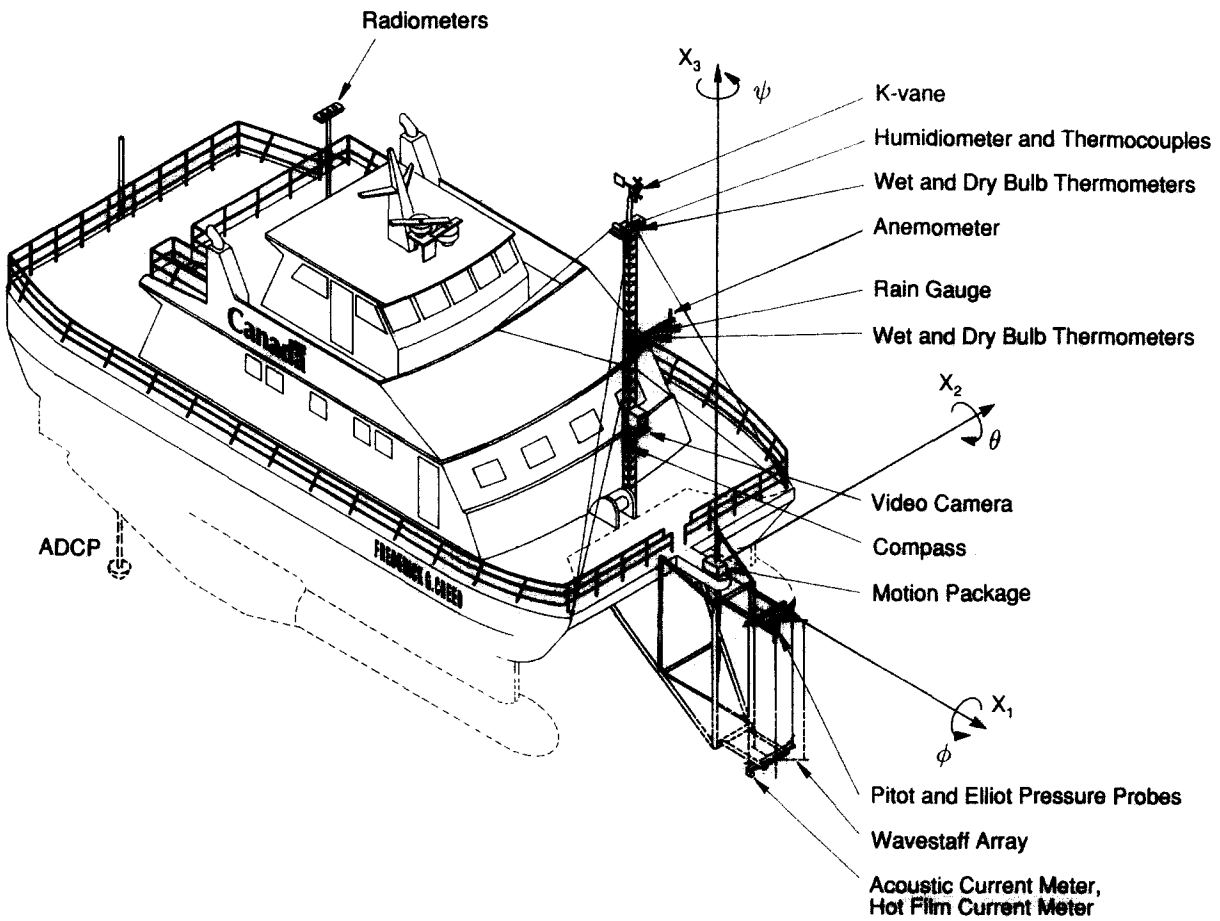

Fig. 3. Sketch of the *Frederick G. Creed* with position of the meteorological mast and the instruments.

and by a gyroscope and two angular accelerometers for roll and pitch. Yaw was measured with both a two-axis flux-gate magnetometer and a digitally encoded magnetic compass. The magnetometer had frequency response commensurate with the accelerometers, but was not available at the beginning of the experiment. On these occasions the slower response magnetic compass was used.

The mean motion of the ship was measured and recorded by three different systems: (i) A Global Positioning System (GPS) for navigation provided recorded data on horizontal velocity and position every second giving speed over the ground. (ii) In the second Intensive Observing Period (IOP2), which was the first cruise of the *Creed*, a small acoustic current meter (Sensordata, Bergen, Norway) was mounted on the bottom of the wave array on the starboard side. It measured speed through the water at a depth of between 1 and 3 m. (iii) In IOP3, or the second cruise of the *Creed*, an Acoustic Doppler Current Profiler (RD Instruments, San Diego, CA) was mounted on the stern of the ship. This instrument yields the horizontal current vector, relative to the ship's velocity, in bins of 4 m thickness starting at a depth of 4 m. These latter two devices give the mean velocity of the ship through the water. In the final calculation of the components of the air velocity, this vector is subtracted from the measured mean horizontal wind relative to the ship. In this way the calculation of the fluxes is not contaminated by the presence of strong currents such as occur in and near the Gulf Stream.

Flux sensors

For turbulent velocity fluctuations we employed a K-Gill unit manufactured by R.M. Young, Co., Traverse City, MI, USA (Ataktürk and Katsaros, 1989; Ataktürk, 1991). It consists of two Gill-propellers mounted 45° above and below the nominal horizontal plane. The two propellers are turned into the mean wind direction by a vane. The vane was especially constructed for the K-Gill in SWADE to have the dimensions 30 cm by 30 cm (larger than the vanes used for single propeller-vane anemometers). Sturdy carbon fibre propellers were used to withstand high wind conditions. The vertical support rod was extended above the junction of the propellers by 36 cm to ensure that the effect on the flow at the propellers due to the rod was the same for both propellers. In addition, the SWADE K-Gill had two tilt sensors mounted at right angles in the 30 cm high cylindrical base of 10 cm diameter. These mean pitch and roll sensors were used only to obtain the mean orientation of the K-Gill to the vertical over a run of 34 min duration. Similarly, the mean output of the horizontal accelerometers yielded the mean tilt of the motion sensing package. Thus the relative orientation of the K-Gill anemometer and the motion package was known. The instantaneous motion of the anemometer was then deduced from the instantaneous motion of the linear and angular accelerometers in the motion package, knowing the horizontal and vertical displacements of the anemometer and motion package and assuming that the ship and its booms and towers moved in translation and rotation like a rigid body. The only deviation from this behavior may be some high frequency vibrations, because the mast was tightly guyed at two levels. The signals themselves illustrate that this was not a problem on the SWATH ship.

Temperature fluctuations were obtained with two copper-constantan and thermocouples of 25 and 50 μm diameter, respectively, with an amplifier of in-house design. Humidity was measured with a Lyman-α humidiometer (AIR Co., Boulder, CO., USA). The thermocouples and humidiometer were housed in a "spray-flinger" whose function was to protect the turbulence sensors from impact by spray or rain. A rotating screen ahead of the sensors flings incoming aerosol particles out of the air stream, and the transducers remain free of salt contamination. It was used successfully in the Humidity EXchange Over the Sea HEXOS experiment during winter storms in 1986 (DeCosmo, 1991; Katsaros et al., 1993). Again, in SWADE we found that after weeks of exposure the thermocouples and the Lyman-α remained clean at the 12 m elevation above m.s.l. The nylon filter on the rotating screen was not even salty to the taste. Cross-comparison of the time series and spectra from the two thermocou-

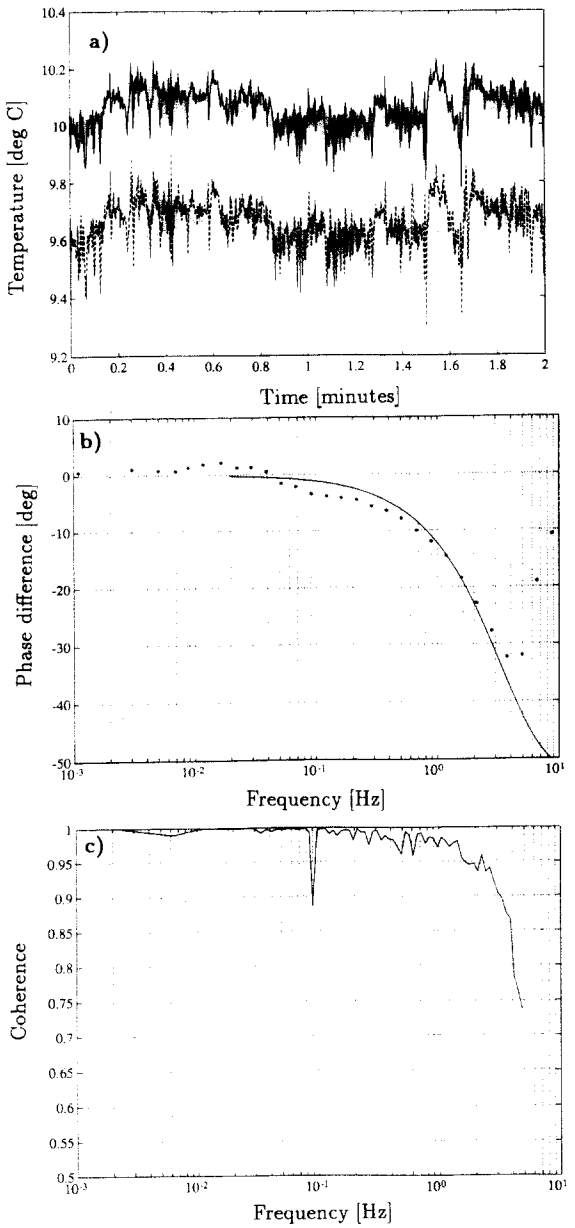

Fig. 4. Illustration of the close agreement between the two thermocouples. (a) time series (top trace offset), (b) (...) observed phase differences and (—) calculate phase differences for time constants differing by a factor of 8, (c) coherence.

ples indicates very close agreement (Fig. 4). Had there been salt contamination of the thermocouples, it is unlikely that they would be contaminated to the same extent and thus respond in the same way. We therefore infer that their close correspondence and lack of tell-tale "ramp" structures (Schmitt et al., 1978) implied that they remained uncontaminated and measured the temperature fluctuations faithfully. The frequency responses of the thermocouples are about 32 and 4 Hz, respectively. Data sampling was at 20 Hz so only minor corrections were necessary for frequency response.

Mean meteorological measurements

Mean wind speed is obtained from the K-Gill propellers after correction for mean ship speed. Temperature and humidity were measured at two levels, 6.9 m and 11.0 m above m.s.l. by the psychrometric method. R.M. Young platinum resistance thermometers were mounted in platelet sun-screens. For the wet-bulbs, large water containers were mounted just below the screens with long wicks reaching in to the screened resistance thermometers. Copper pennies kept algae from growing in the water reservoirs. In addition, a Rotronic humidity sensor with Gortex filter was mounted in its own radiative shield at the 11.0 m height.

Sea surface temperatures (SST's) were obtained from an Acoustic Doppler Current Profiler (ADCP) temperature sensor at about 1 m depth as 5 min averages and from ship intake readings that were calibrated against instantaneous bucket samples. Another source of SST-data was satellite measurements at two channels in the infrared band from the Advanced Very High Resolution Radiometer (AVHRR) on NOAA operational satellites.

Recording systems

Motion sensors, meteorological turbulence sensors and wave gauge data were all sampled by a 32 channel Burr Brown data logger at 20 Hz. Identical 1-pole RC filters with 5 Hz cut-off (3 dB) preceded all the channels. The storage medium was optical disks (WORM drives). Mean meteorological data such as wet and dry bulb temperature pairs, rain rates, pressure and radiation, were collected using a Campbell data logger sampling every 10 s and recording on special cassettes.

Analysis procedures

For turbulent flux calculations, 34 min periods are selected for analysis based on the steadiness of the mean wind. Each signal is then corrected for the effect of the anti-aliasing filter by applying the inverse of the RC (5 Hz) filter function in the frequency domain. The analysis for turbulent fluxes consisted of the following steps:

(a) Comparison of mean tilt from K-Gill pitch and roll tilt sensors with the mean output of the surge and sway accelerometers to establish the relative orientation of the K-Gill and the motion package

The mean K-Gill orientation to the vertical is determined from the mean output of the pitch and roll sensors in the shaft of the K-Gill. The mean orientation of the motion sensors ($\bar{\theta}$, $\bar{\phi}$) is provided by the mean output of the surge and sway accelerometers, $\bar{x}_1$ and $\bar{x}_2$ (Fig. 3).

$$\bar{\theta} = -\sin^{-1}(\bar{\ddot{x}}_1/g) \tag{4}$$

$$\bar{\phi} = \sin^{-1}(\bar{\ddot{x}}_2/g) \tag{5}$$

The means are taken over 34 min and it is assumed that horizontal accelerations on this time scale are negligible compared with the acceleration due to gravity, g; consequently the mean outputs of the accelerometers simply reflect the tilt of the instrument in the gravitational field, $g \sin \bar{\theta}$ or $g \sin \bar{\phi}$.

(b) Correction of K-Gill signals for frequency response of propellers and vane

The correction for the frequency response of the K-Gill propellers follows Hicks (1972) and that of the vane follows MacCready and Jex (1963) or Kenney (1977). The corrections depend on the passage of wind through the sensors and are applied in the form of "distance constants" so that the frequency response varies with wind speed. Consequently the mean wind speed seen by each sensor is first computed. For the propellers this speed is simply determined by multiplying the mean recorded voltage from each propeller by its on-axis calibration. For the vane, the appropriate speed is the speed along the vane-axis. This is determined iteratively at each time step from the propeller's output. The "damping coefficient" and natural (or undamped) wavelength of oscillation for the second order vane

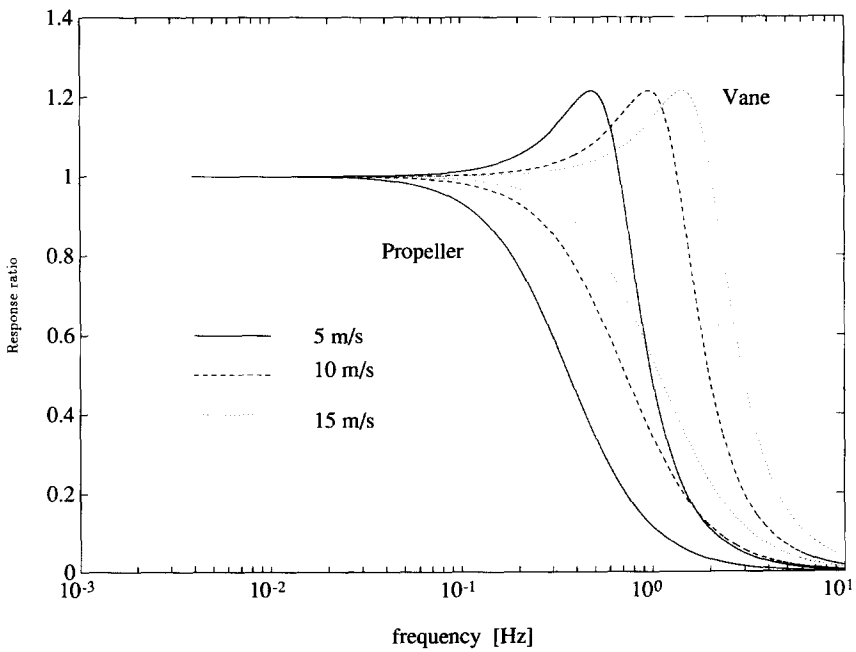

Fig. 5. Propeller and vane response functions.

response correction were obtained in laboratory tests, as was the distance constant for the propellers. These are 0.465, 7.83 m and 2.2 m, respectively. The calculated response functions are shown in Fig. 5.

(c) Correction of Lyman-alpha humidiometer and thermocouples for frequency response reduction caused by the "spray-flinger"

The humidity and temperature signals seen by the sensors inside the spray flinger are smeared out by horizontal diffusion in the 0.6 m pipe of the device. To correct for this effect we use the result of Taylor (1954) concerning longitudinal dispersion in a straight pipe. Taylor found that the impulse response of a straight pipe is Gaussian, so that the spectral amplitude transfer function is:

$$H(f) = e^{-(Bf)^2} \qquad (6)$$

where B depends on the pipe characteristics. In our case the humidiometer and thermocouples inside the pipe and the rotating screen at the entrance do not permit a simple theoretical estimate of B. Instead we estimate B to be 0.15 s by comparing the observed humidity spectrum to the expected Kolmogorov spectrum at high frequencies (Fig. 6).

The humidiometer depends on the absorption of ultraviolet light (Lyman-alpha line), so the frequency response of the instrument is much higher than the 10 Hz limit caused by our sampling rate. The absorption path of the UV beam is transverse to the air flow and the length of the path is only 0.5 cm. Consequently, the filtering associated with averaging along this path is also beyond the range of wavelengths considered here. The signals for both temperature and humidity are corrected for the transfer function Eqn. (6) due to mixing in the pipe.

Unlike the humidiometer, thermocouples have relatively low frequency response, so that additional amplitude and phase corrections in the pass band of interest (0 to 10 Hz) must be considered. The two thermocouples, essentially at the same location in the spray flinger, differed in diameter by a factor of 2 (25 μm and 50 μm) so that the phase shift between them can be used to establish their frequency responses given that the type of response is essentially a single pole RC filter in which the time constant is proportional to the mass of the junction (see Fig. 4). The solid

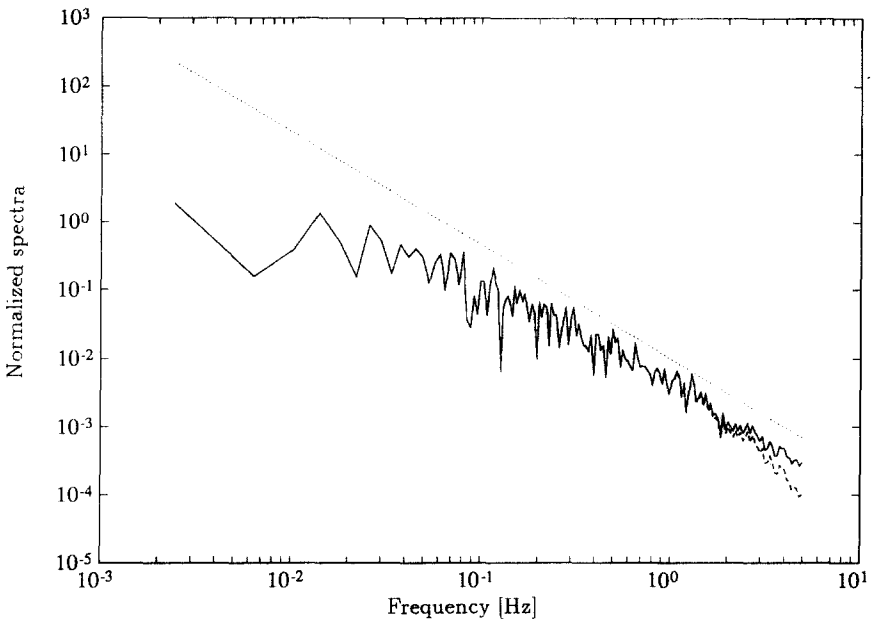

Fig. 6. Spectra of humidity fluctuations. (------) uncorrected and (———) corrected for longitudinal dispersion in the spray flinger. (. . .) $-5/3$ slope expected in the inertial subrange.

line is the best fit phase difference for time constants differing by a factor of 8 (0.005 and 0.04 s respectively). We note that phase differences of a few degrees were seen at 0.5 Hz. Beyond 5 Hz the coherence is low indicating that resolution is lost due to mixing in the spray flinger. Also, flow through the spray flinger is limited to about 3.5 m/s varying slightly with mean wind speed and direction (Katsaros et al., 1993). The thermocouple signals were therefore corrected for single pole RC-filter responses corresponding to time constants of 0.005 and 0.04 seconds.

(d) Computation of the velocity components in the ship reference frame

The response of the K-Gill propellers is a function of their respective angles of attack. This angular response function was obtained through laboratory calibrations of the anemometer (Fig. 7). The angle of attack to which the propellers are subject is related to the tilt of the K-Gill and the vertical angle of the wind. This angle is found iteratively, first assuming the wind to be perpendicular to the K-Gill axis and then calculating the next iteration using the velocities at the top and bottom propellers, the relative wind angle being the arctangent of the velocity components in and normal to the K-Gill axis (see Ataktürk and Katsaros, 1989 for details). In this step we consider only the angle of attack in the vertical. The imperfect response of the vane (Fig. 5) means that the horizontal deviation of the instantaneous wind from the propeller axis will not always be zero. However, deviations of more than 10° are unlikely and produce errors of only a few percent (Fig. 7). This type of error merely attenuates u and w slightly and does not distort the phase between them. The conversion from the K-Gill reference frame to the ship reference frame is then accomplished using the measured azimuth of the K-Gill relative to the bow, and the differences in mean pitch and roll of the K-Gill and the motion package [see section (a) above].

(e) Calculation of the ship's velocity fluctuations

The ship-referenced translational accelerations, recorded by the motion package, are converted to earth-referenced axes by taking into account the pitch, roll and yaw of the ship. (The appropriate coordinate transformation matrix is

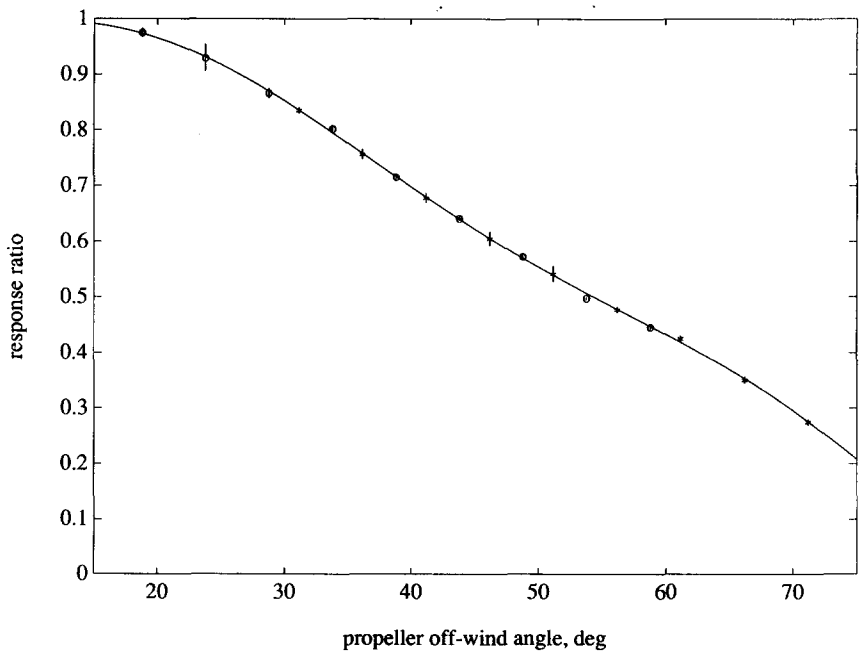

Fig. 7. Measured response of K-Gill with carbon fibre propellers to wind incident at various angles to the propeller axis. The K-Gill unit has the two propellers mounted at 45° off the nominal horizontal direction.

given by Anctil et al., 1993). Integration of these accelerations produces the earth-referenced fluctuations of the ship's translational motion. The ship's mean velocity (over 34 minutes) is derived from another source [see section (h) below].

(f) Computation of the relative air velocity at the K-Gill in earth-referenced coordinates

The relative air velocity measured by the K-Gill is rotated to earth-referenced axes using the instantaneous pitch, roll and yaw of the ship. The ship's translational velocity fluctuations (e) and the velocity induced at the K-Gill by the rotation of the ship are then subtracted to yield the earth-referenced air velocity relative to the mean motion of the ship.

(g) Evaluation of the residual $\overline{w}$ and coordinate rotation required to bring $\overline{w}$ to zero

For each data run $\overline{w}$ is found. If the motion corrections have been done correctly and there is no flow distortion by the ship, $\overline{w}$ should by definition be 0. We found typical values of $\overline{w}$ to be 0.1–0.2 m s^{-1} corresponding to tilts of 1° based on the runs analyzed to date. A 1° tilt of the sensor results in a 10% error in the stress typically. Consequently, we rotate the u and w components to bring $\overline{w}$ to zero through the mean angle, arctan $(\overline{w}/\overline{u})$. If the tilt is due to flow distortion the coordinate rotation results in the wind being evaluated along a mean stream line and for small tilts the errors in the calculated stress and the scalar fluxes are negligible.

(h) Mean ship motion removed from u signal

The helmsman attempted to keep the mean ship velocity and heading constant during each run. The 34-min average horizontal velocity of the ship, as measured by the acoustic current meter, the ADCP or GPS, is subtracted from the earth referenced air velocity relative to the ship to obtain the actual wind velocity.

(i) Co- and auto-spectra of all the turbulence variables calculated and compared to established forms

Spectra and co-spectra calculated from time series of the fluctuating parts of temperature, humidity and velocity signals have been analyzed under ideal conditions and the expected forms of such spectra are well known (e.g., Miyake et al., 1970). Comparison of spectra from the SWATH ship to the typical forms would therefore reveal false contributions due to the ship motions which have characteristic frequencies. These comparisons were routinely done, and good agreement

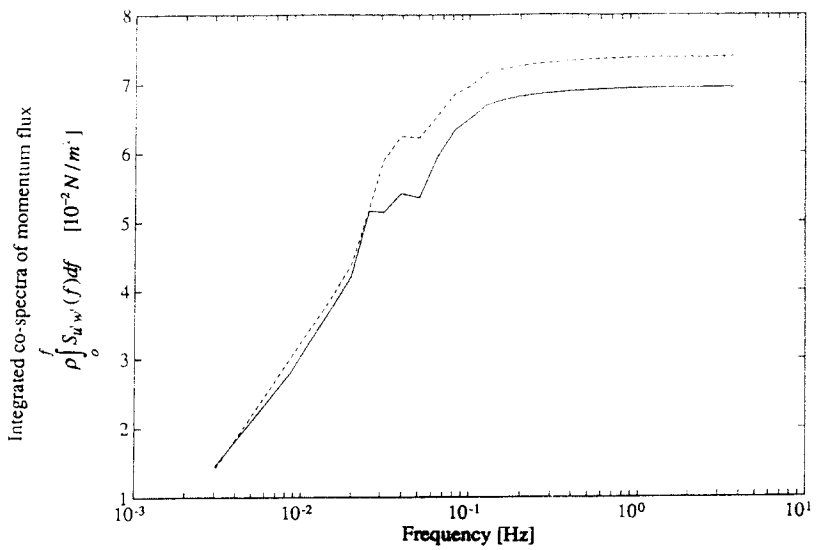

Fig. 8. Integrated co-spectra of momentum flux computed using two different sets of motion sensors.

with "universal spectral forms" was found when the ship was steaming steadily into the wind.

(j) Frequency scale of spectra corrected for Doppler shift due to mean ship motion

In order to account for Doppler shifting of the frequency scale due to mean ship motion, we employ the dimensionless frequency fz/U, as introduced by Miyake et al. (1970). Here f is frequency, z is the height of the anemometer above the water and U the speed of the wind with respect to the ship. U/f corresponds to the length scale of the turbulent eddies measured, whether by a stationary or by a moving sensor.

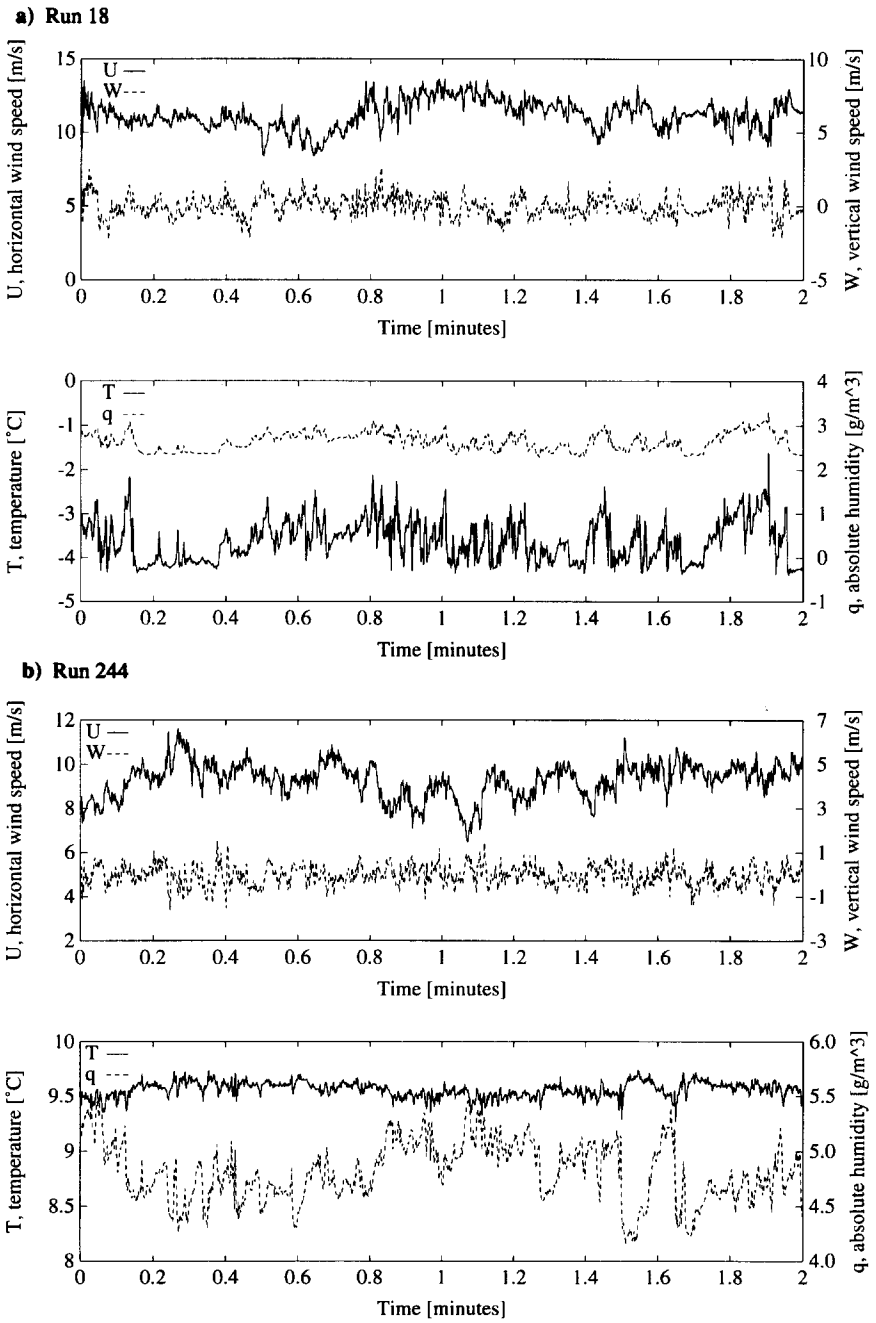

Fig. 9. Time series of velocity components (—u, ---w) and of temperature (— T) and humidity (---q). (a) Run number 18. (b) Run number 244.

(k) Sensitivity tests of u'w', u't', q'w' errors or uncertainties at any stage of the analysis

Computations were repeated using duplicate motion sensors and pre- and post-experiment calibrations to check the effect of errors of this sort on the final results. Figure 8 illustrates the uncertainty by comparing results from two redundant sets of motion sensors. The difference is less than 7%.

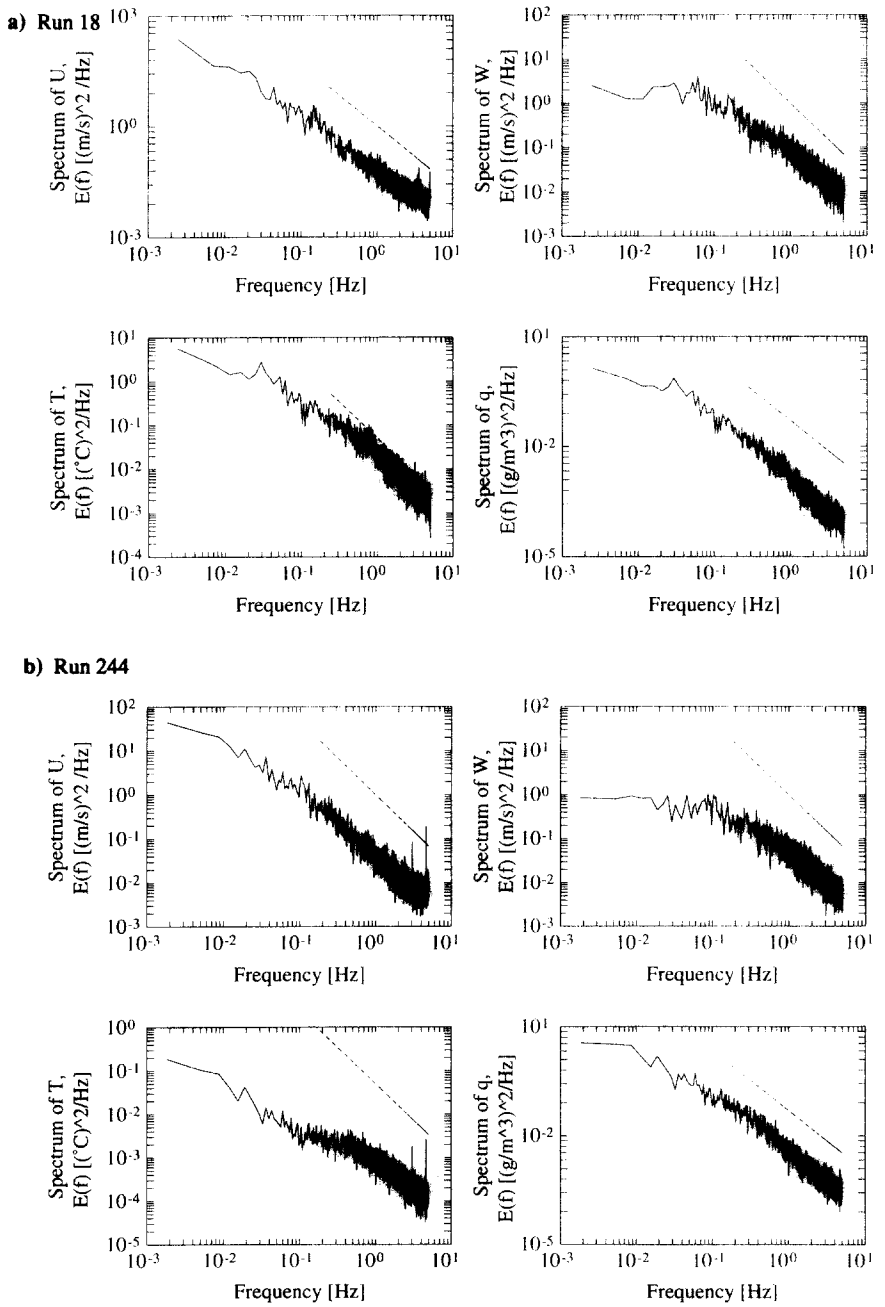

Fig. 10. Spectra of velocity components (u and w) and of scalars T and q. (a) Run 18, (b) Run 244.

(l) Comparison of fluxes determined by eddy correlation with fluxes deduced from the inertial dissipation method via the spectra of u, T and q

From a research tower in near-neutral conditions the inertial dissipation estimates of the turbulent fluxes have been found to give reasonable agreement (within 20% for stress and 25% for sensible heat) with eddy-correlation calculations (e.g., Edson et al., 1991). We used this method (the next section) to test the success of our motion corrections since the inertial subrange

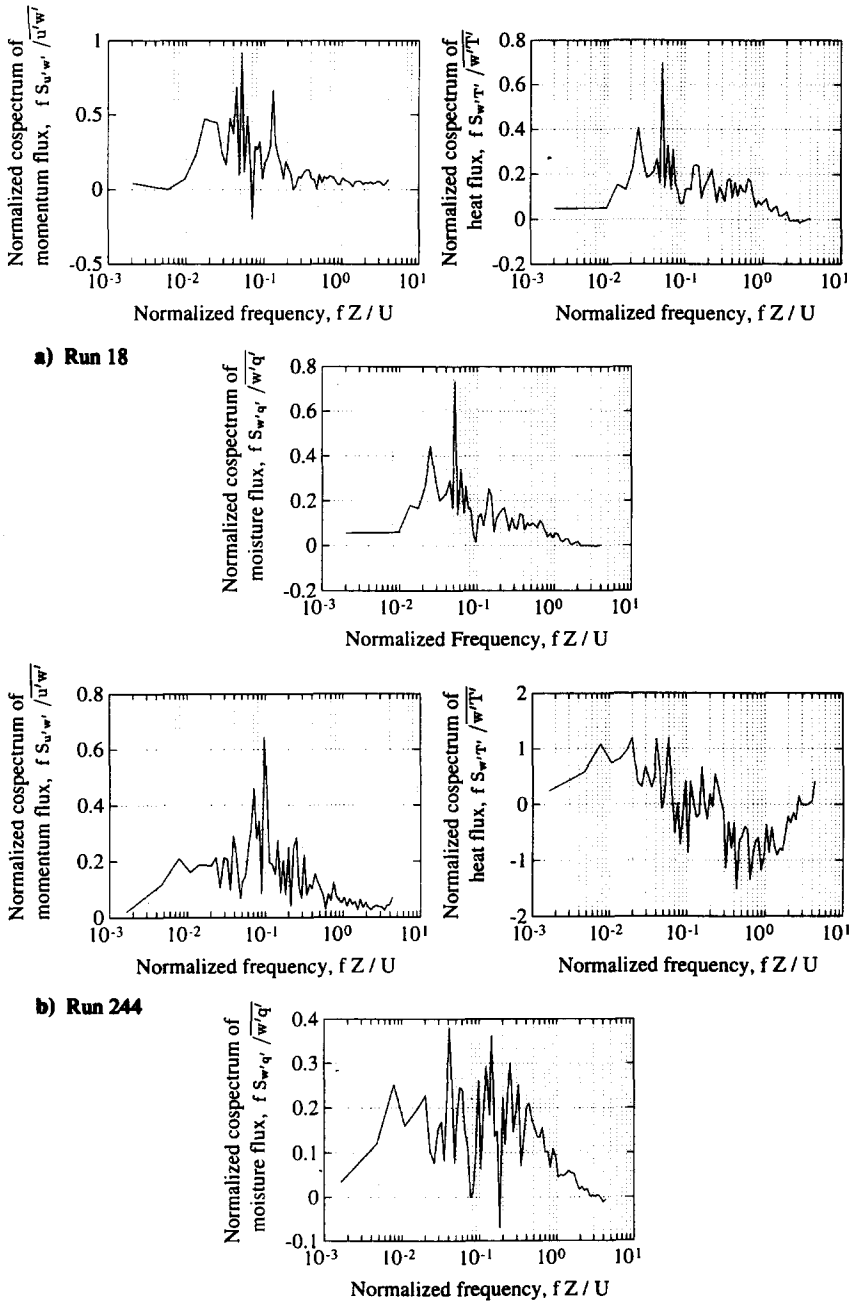

Fig. 11. Normalized co-spectra of momentum ($u'w'$), heat ($w'T'$) and moisture ($w'q'$) fluxes. (a) Run 18, (b) Run 244. Note that the scales are not the same in (a) and (b) and the sign of the mean sensible heat flux is negative for Run 244 (Table 1) resulting in sign reversal after normalization.

TABLE 1

Comparison of fluxes of momentum, heat and moisture calculated by the eddy correlation and inertial dissipation (inertial subrange) methods

Run#	14	18	102	215	244	249	
Date, M/D, 1991	01/22	01/22	02/25	03/05	03/08	03/08	
Start Time, UTC	00:07	17:40	17:10	01:00	00:33	21:23	
$\langle w'u' \rangle_{ec}$	−0.219	−0.240	−0.154	−0.167	−0.158	−0.082	$[(m/s)^2]$
$\langle w'u' \rangle_{diss}$	−0.202	−0.234	−0.209	−0.158	−0.164	−0.104	
$\langle w'T' \rangle_{ec}$	0.052	0.161	0.109	0.039	−0.002	0.035	[°C*(m/s)]
$\langle w'T' \rangle_{diss}$	0.072	0.220	0.121	0.049	0.024	0.065	
$\langle w'q' \rangle_{ec}$	0.022	0.072	0.166	0.095	0.052	0.069	$[(g/m^3)*(m/s)]$
$\langle w'q' \rangle_{diss}$	0.016	0.053	0.143	0.066	0.048	0.070	

The large discrepancy between the eddy correlation and the inertial subrange estimates of sensible heat flux $\langle w'T' \rangle$ evident in Run 244 can be explained by the division of the $w'T'$ covariance between a low frequency downward flux and a high frequency upward flux (see Fig. 11b).

method is less sensitive to low frequency ship movements. The formulations used and the values of the empirical coefficients are taken from Large and Pond (1982).

Results

In order to demonstrate that indeed this complicated analysis trail leads to reasonable flux estimates, we show a few examples and compare with inertial dissipation estimates. Complete analysis of the turbulent fluxes, especially the wind stress measured on *The Creed* in SWADE and their relations to the varying wave field, PBL height, and synoptic or mesoscale structures will be pursued and the results presented in future publications.

Time series of u, w, T and q for two runs are seen in Fig. 9 a,b, the corresponding auto-spectra in Fig. 10 a,b, and the co-spectra of $u'w'$, $w'T'$ and $w'q'$ in Fig. 11 a,b. The run illustrated by the top (a) part of these figures corresponds to a cold air outbreak, while the lower (b) figures are for an exceptional case with small net heat flux. The auto-spectra all present the classical $-5/3$ slope at high frequencies (e.g., Kaimal et al., 1972) except the temperature spectrum of Fig. 10b. The co-spectra have large fluctuations at low frequencies which is typical for all turbulence realizations, but they are again of "classical" shape with no evidence of contamination from the ship motion. The heat flux co-variance spectrum of Fig. 11b shows a negative low frequency lobe. (Because of the normalization with the mean heat flux, which is small and negative, the numbers are large and positive at the low frequency end of Fig. 11b.) In this case low frequency motions carry heat downward while high frequencies carry heat upwards. This behavior has been observed in previous air–sea flux studies (Donelan and Miyake, 1973). The water vapor spectrum does not exhibit any similar "odd" behavior since the q-gradient is strongly upward directed at all scales.

In Table 1 comparison of the eddy correlation and the inertial subrange estimates of the co-variances shows generally excellent agreement between these two methods. The differences are of the order of 20–30%, which is typical of such comparisons (e.g., Edson et al., 1991). Only for the sensible heat flux of column 5 is the difference significantly larger. For this case the discrepancy can be explained as being due to a failure of the assumptions required for use of the inertial subrange method, namely that production of turbulence equals dissipation and that turbulent energy is transferred by a cascade from low to high frequencies. For the case of column 5 corresponding to the co-spectrum of Fig. 11b for $w'T'$, where the low frequencies carry heat downwards while the high frequencies carry heat upwards, these two fluxes almost negate each other exactly. The inertial subrange of the autospec-

trum for temperature of Fig. 10b is restricted to very high frequencies, another indication that the inertial dissipation method may be inappropriate.

Discussion

The eddy correlation method for turbulent flux determination is the preferred method, because it simply uses the definitions of the turbulent fluxes. This method has not been used from ships at high wind speeds, because the movement of the ship introduces fluctuations in the measured quantities (wind, temperature and humidity) that lie in the range of the flux-carrying turbulent scales. In addition the bulk of a ship introduces flow distortions, which may be detrimental. In principle, if all the details of the ship's motion are carefully measured the effects can be removed from the turbulence measurements (principally the velocity components). All these measurements are difficult to make and high speed recording of a large number of channels is required.

We have successfully determined the turbulent fluxes by the eddy correlation method from a small SWATH ship, whose flow distortion was minimal at the position of our sensors. In this paper the complex analysis trail has been described in some detail, since it appears to be the first time that this procedure has been carried out.

Repeated calculations of the motion corrections using different sets of instruments produce differences in the calculated flux of momentum of less than 7%. This uncertainty is well below the typical sampling variability for half-hourly averages, and may thus be taken as a measure of the validity of the motion correction procedures.

The measured flow distortion in terms of the upsweep angle at the position of the K-Gill anemometer, 12 m above the sea, 8 m above the foredeck was 0.5 to 1 degree. It is indicative of the very small effect of the SWATH ship on the flow. This order of magnitude distortion of the streamlines around an obstacle is typical even for the "cleanest" turbulence experiment and may, in fact, be caused by the support structure of the anemometer (e.g. DeCosmo, 1991; Oost et al., 1993).

Finally, we have compared our eddy correlation estimates of the turbulent fluxes to the inertial dissipation method, since the latter is an alternative method for measuring fluxes from ships or buoys. The dissipation method and the eddy correlation method have not been compared for data obtained on a moving platform before. (The two methods have, however, often been compared for data obtained on stable platforms.) Our preliminary sample of six runs showed that the methods agreed on average (mean of absolute percent error) to within 12% for momentum. The average errors for water vapor and heat fluxes were 20% and 31%, respectively. The case (Run 244) in which the heat flux is oppositely directed at large and small scales is omitted from this calculation since the inertial dissipation method is clearly invalid under these circumstances. By way of "calibrating" the quality of this comparison we note that Edson et al. (1991), in a similar comparison using data collected on a fixed tower, found agreement of 20% and 25% for momentum and sensible heat flux, respectively. We emphasize that the differences between the methods are most likely due to restrictive conditions of validity of the inertial dissipation method.

This paper describes the fundamental measurements. We now intend to seek explanations for variability of these fluxes in terms of the steadiness of the synoptic situation, boundary layer structures, horizontal inhomogeneity and the type of sea state.

Acknowledgments

We appreciate the support for our SWADE work from the Office of Naval Research Grant N00014-89-1785 to the University of Washington and Grant N00014-88-J-1028 to the National Water Research Institute; additional support for the use of the SWATH ship was provided jointly by the Office of Naval Research, National Aeronautics and Space Administration and the Coastal Engineering Research Center of the U.S. Army. We thank Drs. A. Brandt (ONR), W. Patzert (NASA) and C. Vincent (CERC) for their willingness to support the use of the SWATH ship as a replacement for the spar buoy. Their foresight

and confidence in the scientific team turned the tide following the set-back of losing the spar. Steve Peck (Fisheries and Oceans, Canada) facilitated the modification and use of the SWATH ship. Captain Sebastian Bodman of the *Frederick G. Creed* and his crew were enthusiastic and helpful partners in the data collection. Fellow scientists on the ship, Gene Terray, Charlie Flagg and Katherine Howard advised and assisted with data logging and support measurements. Technical development by Niels Madsen, Joe Gabriele, Frederick Weller and Noel Cheney is much appreciated as is the assistance with the data analysis of Neal Johnson, Katherine Howard and Ralph Monis at the University of Washington. We are grateful to Hans Graber of the University of Miami for satellite SST maps derived from AVHRR data and to Janet Meadows who ably typed the manuscript.

References

Anctil, F., Donelan, M.A., Drennan, W.M. and Graber, H.C., 1993. Eddy correlation measurements of air-sea fluxes from a Discus Buoy. J. Atmos. Ocean. Tech., (submitted).

Ataktürk, S.S. and Katsaros, K.B., 1989. The K-Gill: a twin propeller-vane anemometer for measurements of atmospheric turbulence. J. Atmos. Ocean. Tech., 6, 509–515.

Ataktürk, S.S., 1991. Characterization of Small-Scale Roughness Elements on a Water Surface. Ph.D. Thesis. Dep. Atmos. Sci., Univ. Washington, Seattle, WA 98195, 196 pp.

Bradley, E.F., Coppin, P.A. and Godfrey, J.S., 1991. Measure of sensible and latent heat flux in the equatorial Pacific Ocean. J. Geophys. Res., 96: 3375–3389.

DeCosmo, J., 1991. Air–Sea Exchange of Momentum, Heat, and Water Vapor Over Whitecap Sea States. Ph.D. Thesis, Dep. Atmos. Sci. Univ. Washington, Seattle, WA 98195, 212 pp.

Donelan, M.A., 1990. Air–sea interaction. In: B. LeMehaute and D. Hanes (Editors), The Sea: Ocean Engineering Science, 9.: 239–292.

Donelan, M.A. and Miyake, M., 1973. Spectra and fluxes in the boundary layer of the trade-wind zone. J. Atmos. Sci., 30: 444–464.

Edson, J.B., Fairall, C.W., Mestayer, P.G. and S.E. Larsen, 1991. A study of the inertial-dissipation method for computing air–sea fluxes. J. Geophys. Res., 96: 10,689–10,711.

Hicks, B.B., 1972. Propeller anemometers as sensors of atmospheric turbulence. Boundary-Layer Meteorol., 3: 214–228.

Fairall, C.W. and Larsen, S.E., 1986. Inertial dissipation methods and turbulent fluxes at the air–ocean interface. Boundary-Layer Meteorol., 34: 287–301.

Kaimal, J.C., Wyngaard, J., Izumi, Y. and Coté, O.R., 1972. Spectral characteristics of surface layer turbulence. Q.J. R. Meteorol. Soc., 98: 563–589.

Katsaros, K.B., DeCosmo, J., Anderson, R.J., Smith, S.D., Kraan, R., Oost, W., Uhlig, K., Mestayer, P., Smith, M.H., de Leeuw, G. and Lind, R.J., 1993. Measurements of humidity and temperature in the marine environment. J. Atmos. Ocean Techn. (in press).

Kenney, B., 1977. Response characteristics affecting the design and use of current direction vanes. Deep-Sea Res., 24: 289–300.

Large, W.G. and Pond, S., 1982. Sensible and latent heat flux measurements over the ocean. J. Phys. Ocean., 12: 464–482.

MacCready, P.B. and Jex, H.R., 1963. Response characteristics and meteorological utilization of propeller and vane wind sensors. J. Appl. Meteorol., 3: 182–193.

Miyake, M., Stewart, R.W. and Burling, R.W., 1970. Spectra and cospectra of turbulence over water. Q.J. R. Meteorol. Soc., 96: 138–143.

Mitsuta, Y. and Fujitani, T., 1974. Direct measurement of turbulent fluxes on a cruising ship. Boundary-Layer Meteorol., 6: 203–217.

Oost, W.A., Fairall, C.W., Edson, J.B., Smith, S.D., Anderson, R.J., Wills, J.A.M., Katsaros, K.B. and DeCosmo, J., 1991. Flow distortion calculations and their application in HEXMAX.J. Atmos. Ocean. Tech. (in press).

Schmitt, K.F., Friehe, C.A. and Gibson, C.H., 1978. Humidity sensitivity of atmospheric temperature sensors by salt. J. Phys. Ocean., 8: 151–161.

Smith, S.D., Anderson, R.J., Oost, W.A., Kraan, C., Maat, N., DeCosmo, J., Katsaros, K.B., Davidson, K.L., Bumke, K., Hasse, L. and Chadwick, H., 1992. Sea surface wind stress and drag coefficients: the HEXOS results. Boundary-Layer Meteorol., 60: 109–142.

Taylor, G.I., 1954. The dispersion of matter in turbulent flow through a pipe. Proc. R. Soc. London Ser. A, 223: 446–468.

Weller, R.A., Donelan, M., Briscoe, M. and Huang, N.E., 1991. Riding the crest: A tale of two experiments. Bull. Am. Meteorol. Soc., 72: 163–183.